Electronic Supplementary Information – Revealing the role of intrinsic point defects in stability of halide double perovskite $Cs_2AgBiBr_6$

Il-Chol Ri, Chun-Son Ri, Song-Hyon Yu, Son-Hyok Jo, Song-Hyok Choe, Chol-Jun Yu*

Chair of Computational Materials Design (CMD), Faculty of Materials Science, Kim Il Sung University, Ryongnam-Dong, Taesong District, Pyongyang, PO Box 76, Democratic People's Republic of Korea

Computational detail for defect

The pseudopotential plane wave method was adopted, as implemented in the Quantum ESPRESSO package [1]. Primitive unit cell of cubic $Cs_2AgBiBr_6$, containing 10 atoms, was used for electronic structure calculations with the $(6 \times 6 \times 6)$ k-points and HSE06 hybrid exchange-correlation functional [2]. For defective systems, we constructed $3 \times 3 \times 3$ supercells (270 atoms) and performed atomic relaxations with an atomic force threshold of 5×10^{-4} Ry/Bohr using the Γ point and PBE functional [3]. Based on the PBE-optimized supercells, we finally performed the self-consistent field (SCF) calculations using the HSE06 functional to get the total energy. We note that the PBE calculations provide sufficiently accurate results on forces, structures, and band dispersion, but underestimates band gaps. Therefore, this method was proved to be a reliable method to balance the computational cost and the calculation accuracy. The kinetic cut-off energies were 50 and 500 Ry for wave functions and electron density, respectively. The formation energies of the intrinsic point defects were evaluated under the chemical potential conditions [4]. Computational details are provided in the supplementary material. Then, we used $2 \times 2 \times 2$ supercells for vacancy-mediated ion migrations, for which the activation energies were determined by applying the nudged elastic band (NEB) method [5].

The formation energy of defect X with charge state q is calculated as follows,

$$E_f(X^q) = E_{\text{tot}}(X^q) - E_{\text{tot}}(\text{perf}) + \textstyle\sum_i n_i\mu_i + q(\mu_e + E_{\text{VBM}}) + E^q_{\text{corr}}, \tag{S1}$$

where $E_{\text{tot}}(X^q)$ and $E_{\text{tot}}(\text{perf})$ are the total energies of the defect and perfect supercells, and n_i and μ_i indicate the number of atoms added into ($n_i < 0$) or removed from ($n_i > 0$) the perfect supercell and the atomic chemical potential of species i. μ_e is the electronic chemical potential or the Fermi level, *i.e.*, the energy of the electron reservoir, and is referenced to the valence band maximum (VBM) energy E_{VBM}, thereby changing from 0 to the band gap E_g of the perfect bulk. The correction term E^q_{corr} denotes the effect of finite size of periodic supercells on the total energy of the charged defect supercell, and can be calculated within the monopole approximation by $E^q_{\text{corr}} \approx \alpha q^2/\varepsilon L$, where ε is the static dielectric constant, α the Madelung constant and L the lattice constant [6, 7].

Once the formation energy of the defect is calculated, the concentration of the defect X in thermal equilibrium can be determined at temperature T by the following relation [4],

$$c(X) = N_{\text{sites}} N_{\text{conf}} \exp\left(\frac{-E_f(X)}{k_B T}\right), \tag{S2}$$

where N_{sites} is the number of defect-incorporated sites in the lattice per unit cell volume, and N_{conf} is the number of equivalent configuration per site. It is clear that the lower formation energy could lead to higher concentration of defect.

The chemical potential μ_i, representing the free energy required to exchange particles between the reservoir with infinite amounts of energy and particles and the corresponding system, can be defined as $\mu_i = E_i^{\text{bulk}} + \Delta\mu_i$, where E_i^{bulk} is the total energy of the elementary bulk solid per atom. For the $Cs_2AgBiBr_6$ compound under study, the reservoir solid materials are referenced to fcc Cs metal (space group $Fm\bar{3}m$), fcc Ag metal ($Fm\bar{3}m$), trigonal Bi metal ($R3m$), and monoclinic Br solid ($Cmca$);

$$\Delta\mu_{\text{Cs}} = \mu_{\text{Cs}} - E^{\text{fcc}}_{\text{Cs}}, \;\; \Delta\mu_{\text{Ag}} = \mu_{\text{Ag}} - E^{\text{fcc}}_{\text{Ag}}, \;\; \Delta\mu_{\text{Bi}} = \mu_{\text{Bi}} - E^{R3m}_{\text{Bi}}, \;\; \Delta\mu_{\text{Br}} = \mu_{\text{Br}} - E^{Cmca}_{\text{Br}}. \tag{S3}$$

The chemical potentials are not independent but variable, being required to meet the thermodynamic constraints related with the synthesis condition in experiment. Firstly, to avoid precipitating elementary bulk Cs, Ag, Bi and Br solid during the synthesis, the following inequalities should be satisfied;

$$\Delta\mu_{\text{Cs}} \le 0, \;\; \Delta\mu_{\text{Ag}} \le 0, \;\; \Delta\mu_{\text{Bi}} \le 0, \;\; \Delta\mu_{\text{Br}} \le 0. \tag{S4}$$

These sets an upper bound on the chemical potentials. Secondly, the competing binary compounds A_xB_y (A, B = Cs, Ag, Bi, Br) should not be formed as well, requiring the chemical potentials to meet the following constraint,

*Corresponding author: Chol-Jun Yu, Email: cj.yu@ryongnamsan.edu.kp

$$x\Delta\mu_{\mathrm{A}} + y\Delta\mu_{\mathrm{B}} \leq \Delta H_f(\mathrm{A}_x\mathrm{B}_y) \approx E^{\mathrm{bulk}}_{\mathrm{A}_x\mathrm{B}_y} - (xE^{\mathrm{bulk}}_{\mathrm{A}} + yE^{\mathrm{bulk}}_{\mathrm{B}}), \tag{S5}$$

where $\Delta H_f(\mathrm{A}_x\mathrm{B}_y)$ is the formation enthalpy that can be approximated to be the DFT total energy difference while ignoring the negligible entropic and volumetric contributions. Thirdly, the formation of ternary compounds $\mathrm{A}_x\mathrm{B}_y\mathrm{C}_z$ should also be prevented, leading the following constraints,

$$x\Delta\mu_{\mathrm{A}} + y\Delta\mu_{\mathrm{B}} + z\Delta\mu_{\mathrm{C}} \leq \Delta H_f(\mathrm{A}_x\mathrm{B}_y\mathrm{C}_z) \approx E^{\mathrm{bulk}}_{\mathrm{A}_x\mathrm{B}_y\mathrm{C}_z} - (xE^{\mathrm{bulk}}_{\mathrm{A}} + yE^{\mathrm{bulk}}_{\mathrm{B}} + zE^{\mathrm{bulk}}_{\mathrm{C}}). \tag{S6}$$

Lastly, stable existence of $\mathrm{Cs_2AgBiBr_6}$ requires the following equation;

$$2\Delta\mu_{\mathrm{Cs}} + \Delta\mu_{\mathrm{Ag}} + \Delta\mu_{\mathrm{Bi}} + 6\Delta\mu_{\mathrm{Br}} = \Delta H_f(\mathrm{Cs_2AgBiBr_6}) \approx E^{Fm\bar{3}m}_{\mathrm{Cs_2AgBiBr_6}} - (2E^{fcc}_{\mathrm{Cs}} + E^{fcc}_{\mathrm{Ag}} + E^{R3m}_{\mathrm{Bi}} + E^{Cmca}_{\mathrm{Br}}). \tag{S7}$$

This gives a lower bound on the chemical potentials. All these constraints can determine the range of Cs, Ag, Bi and Br chemical potentials in which the host compound $\mathrm{Cs_2AgBiBr_6}$ is thermodynamically stable.

The Fermi level μ_e, *i.e.*, the electronic chemical potential, is not a free parameter as well. In fact, Eqs. (S1) and (S2) can be formed for all intrinsic defects and impurities in the compound. Then, the equations should be solved in a self-consistent way with the charge neutrality condition for free electrons in the conduction bands and free holes in the valence bands as follows,

$$\textstyle\sum_i c_i q_i - n_e + n_h = 0, \tag{S8}$$

where c_i and q_i are the concentration and charge of defect or impurity, and n_e and n_h are the concentrations of free electrons and free holes, respectively.

The lattice vectors and positions of atoms in the unit cell of $\mathrm{Cs_2AgBiBr_6}$ are provided in Table S4. The typical input file of pw.x code for atomic relaxations in the supercell is provided below.

```
 &CONTROL
    calculation = 'relax',
   restart_mode = 'from_scratch',
         outdir = 'relax',
         prefix = 'relax',
     pseudo_dir = '/home/pub/pseudo/upf_files/gbrv/',
  forc_conv_thr = 5.0D-4,
        nstep   = 200,
        tstress = .true.,
        tprnfor = .true.,
 /
 &SYSTEM
    ibrav = 0, celldm(1) = 1.889726342,
    ntyp = 4, nat  = 269,
    ecutwfc = 50, ecutrho = 500,
    input_dft = 'PBE',
    tot_charge = +2,
    occupations = 'smearing', smearing = 'm-p', degauss = 0.02
 /
 &electrons
    electron_maxstep = 100,
            conv_thr = 1.0d-7,
         mixing_beta = 0.7
 /
 &ions
    ion_dynamics = 'bfgs',
 /

ATOMIC_SPECIES
  Cs  132.906    cs_pbe_v1.uspp.F.UPF
  Bi  208.980    bi_pbe_v1.uspp.F.UPF
  Ag  107.868    ag_pbe_v1.4.uspp.F.UPF
  Br   79.904    br_pbe_v1.4.uspp.F.UPF

K_POINTS {automatic}
2 2 2 1 1 1

CELL_PARAMETERS (alat= 1.0)
  24.33769989         0.00000000         0.00000000
```

```
  12.16884994        21.07706637         0.00000000
  12.16884994         7.02568879        19.87164875

ATOMIC_POSITIONS (crystal)
...
```

For the SCF calculations of relaxed structure, the XC functional *PBE* is changed to *HSE* and the k-point setting is changed to "*K_POINTS gamma*". The typical input file of neb.x code for NEB simulation is as follow.

```
BEGIN
BEGIN_PATH_INPUT
&PATH
  restart_mode      = 'restart'
  string_method     = 'neb',
  nstep_path        = 2000,
  ds                = 1.D0,
  opt_scheme        = 'broyden',
  num_of_images     = 7,
  k_max             = 0.3D0,
  k_min             = 0.2D0,
  path_thr          = 0.05D0,
  minimum_image     = .true.,
  CI_scheme         = 'auto',
  first_last_opt    = .false.,
  use_freezing      = .true.
/
CLIMBING_IMAGES
 4
END_PATH_INPUT

BEGIN_ENGINE_INPUT
 &CONTROL
    prefix     = 'agmig'
    pseudo_dir = '/home/pub/pseudo/upf_files/gbrv/',
 /
 &SYSTEM
    ibrav = 0,
    celldm(1) = 1.889726342,
    ntyp = 4, nat  = 268,
    ecutwfc = 50, ecutrho = 500,
    input_dft = 'PBE',
    occupations = 'smearing', smearing = 'm-p', degauss = 0.02
 /
 &electrons
    electron_maxstep = 100,
            conv_thr = 1.0d-7,
         mixing_beta = 0.7
 /

ATOMIC_SPECIES
  Cs  132.906    cs_pbe_v1.uspp.F.UPF
  Bi  208.980    bi_pbe_v1.uspp.F.UPF
  Ag  107.868    ag_pbe_v1.4.uspp.F.UPF
  Br   79.904    br_pbe_v1.4.uspp.F.UPF

CELL_PARAMETERS (alat= 1.0)
  24.33769989         0.00000000         0.00000000
  12.16884994        21.07706637         0.00000000
  12.16884994         7.02568879        19.87164875

K_POINTS gamma

BEGIN_POSITIONS
```

```
FIRST_IMAGE
ATOMIC_POSITIONS (crystal)
...
LAST_IMAGE
ATOMIC_POSITIONS (crystal)
...
END_POSITIONS

END_ENGINE_INPUT
END
```

The atomic positions in the supercells are provided as separate files (cif).

Tables and figures for additional data

Table S1. Ultrasoft pseudopotentials from GBRV library [8] with valence electron configuration for elements and the structural phase and binding energy per atom (E_b) in their simple substances.

Element	Pseudopotential	Configuration	Structure (space group)	E_b (eV/atom)
Cs	cs_pbe_v1.uspp.F.UPF	$5s^2 5p^6 6s^1$	fcc ($Fm\bar{3}m$)	−5.0618 (−5.12)
Ag	ag_pbe_v1.4.uspp.F.UPF	$4s^2 4p^6 4d^{10} 5s^1$	fcc ($Fm\bar{3}m$)	−1.9267
Bi	bi_pbe_v1.uspp.F.UPF	$5d^{10} 6s^2 6p^3$	trigonal ($R3m$)	−1.3131
Br	br_pbe_v1.4.uspp.F.UPF	$4s^2 4p^5$	orthorhombic ($Cmca$)	−1.0667

Table S2. ICSD number, space group and formation energies E_f of all competing binary and ternary compounds in comparison with those from the Materials Project (MP) [11] for the quaternary Cs-Ag-Bi-Br system.

			E_f (eV/atom)	
Compound	ICSD	Space group	This work	MP
Cs_3Bi	58769	$Fm\bar{3}m$	−0.324	−0.466
Cs_3Bi_2	240017	$C12/c1$	−0.366	−0.491
Cs_5Bi_4	240005	$C12/m1$	−0.395	–
CsBi	55067	$P121/C1$	−0.368	−0.511
$CsBi_2$	58771	$Fd\bar{3}ms$	−0.316	−0.390
CsBr	22174	$Pm\bar{3}m$	−1.803	−2.014
CsBr	61516	$Fm\bar{3}m$	−1.778	−2.009
$CsBr_3$	22130	$Pmnb$	−0.990	−1.098
Ag_3Bi	104389	$Fm\bar{3}m$	0.072	0.147
AgBi	104390	$P63/mmc$	0.152	–
AgBr	65061	$Fm\bar{3}m$	−0.341	−0.451
AgBr	56549	$P121/m1$	−0.342	−0.409
BiBr	1560	$C12/m1$	−0.497	−0.743
$BiBr_3$	100294	$C12/m1$	−0.777	−1.170
$BiBr_3$	100293	$P121/a1$	−0.747	−1.111
$CsAgBr_2$	40480	$Ccmm$	−1.103	–
$CsAgBr_2$	150301	$Cmcm$	−1.104	−1.343
$CsAgBr_2$	150302	$P4/nmmz$	−1.111	−1.352
Cs_2AgBr_3	150288	$Pnma$	−1.364	−1.599
$Cs_3Bi_2Br_9$	1142	$P\bar{3}m1$	−1.280	−1.604
$Cs_3Bi_2Br_9$	96723	$C12/c1$	−1.275	−1.603
$Cs_2AgBiBr_6$	–	$Fm\bar{3}m$	−1.157	−1.456

Table S3. Chemical potentials of elements according to the Br-rich, -moderate and -poor conditions (unit: eV).

Condition	Points	$\Delta\mu_{Br}$	$\Delta\mu_{Cs}$	$\Delta\mu_{Ag}$	$\Delta\mu_{Bi}$
Br-rich	A	−0.1	−3.738	−0.588	−2.905
	B	−0.1	−3.685	−0.588	−3.011
	C	−0.1	−3.685	−0.616	−2.983
Br-moderate	A	−0.3	−3.540	−0.386	−2.303
	B	−0.3	−3.447	−0.386	−2.489
	C	−0.3	−3.416	−0.447	−2.490
Br-poor	A	−0.6	−3.238	−0.086	−1.407
	B	−0.6	−3.147	−0.086	−1.589
	C	−0.6	−3.116	−0.149	−1.588

Table S4. Lattice vectors a, b and c in Å unit and positions of atoms in crystal coordinates in the primitive unit cell of $Cs_2AgBiBr_6$.

	x	y	z
a	8.11257168	0.00000000	0.00000000
b	4.05628584	7.02569316	0.00000000
c	4.05628584	2.34189772	6.62484787
Cs	0.25	0.25	0.25
Cs	0.75	0.75	0.75
Ag	0.50	0.50	0.50
Bi	0.00	0.00	0.00
Br	0.74865495	0.25132380	0.25136631
Br	0.25134505	0.74867620	0.74863369
Br	0.25132380	0.74865495	0.25136631
Br	0.74867620	0.25134505	0.74863369
Br	0.25134505	0.25134505	0.74863369
Br	0.74865495	0.74865495	0.25136631

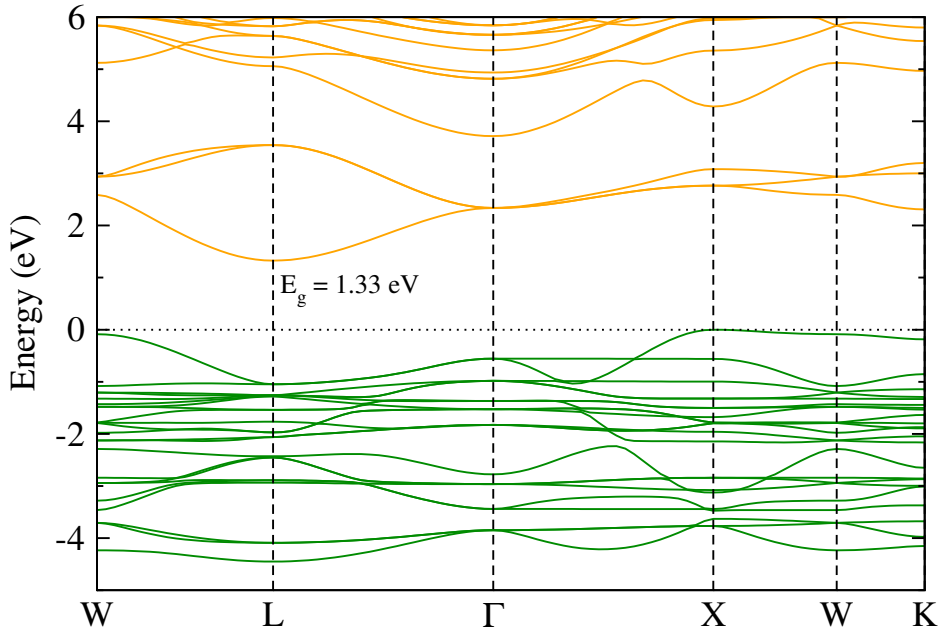

Fig. S1 The electronic band structure calculated by using the PBE exchange-correlation functional.

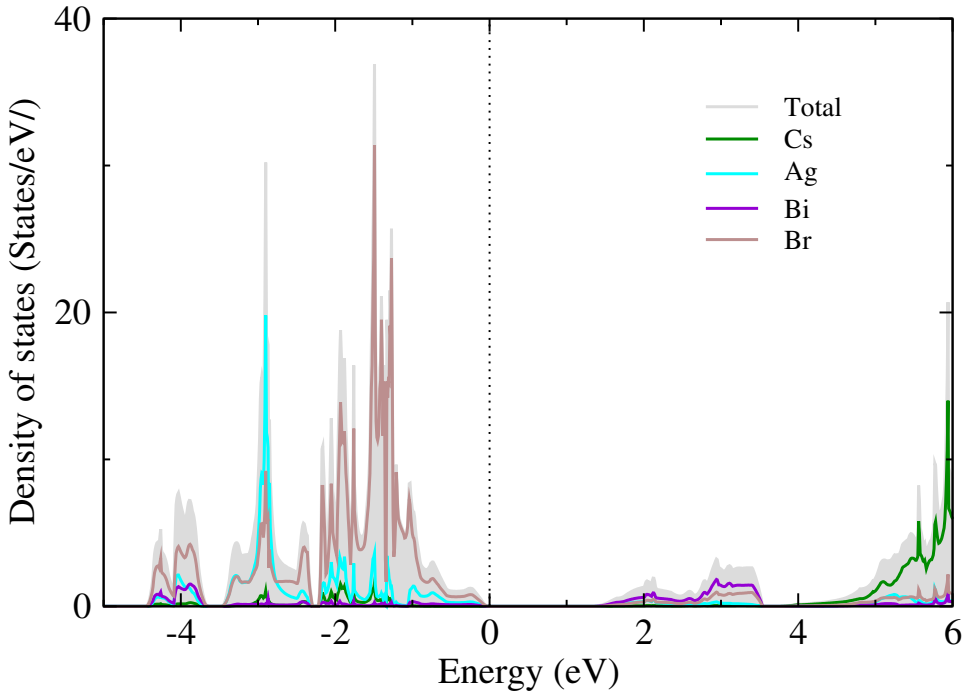

Fig. S2 The total density of states calculated by using the PBE exchange-correlation functional.

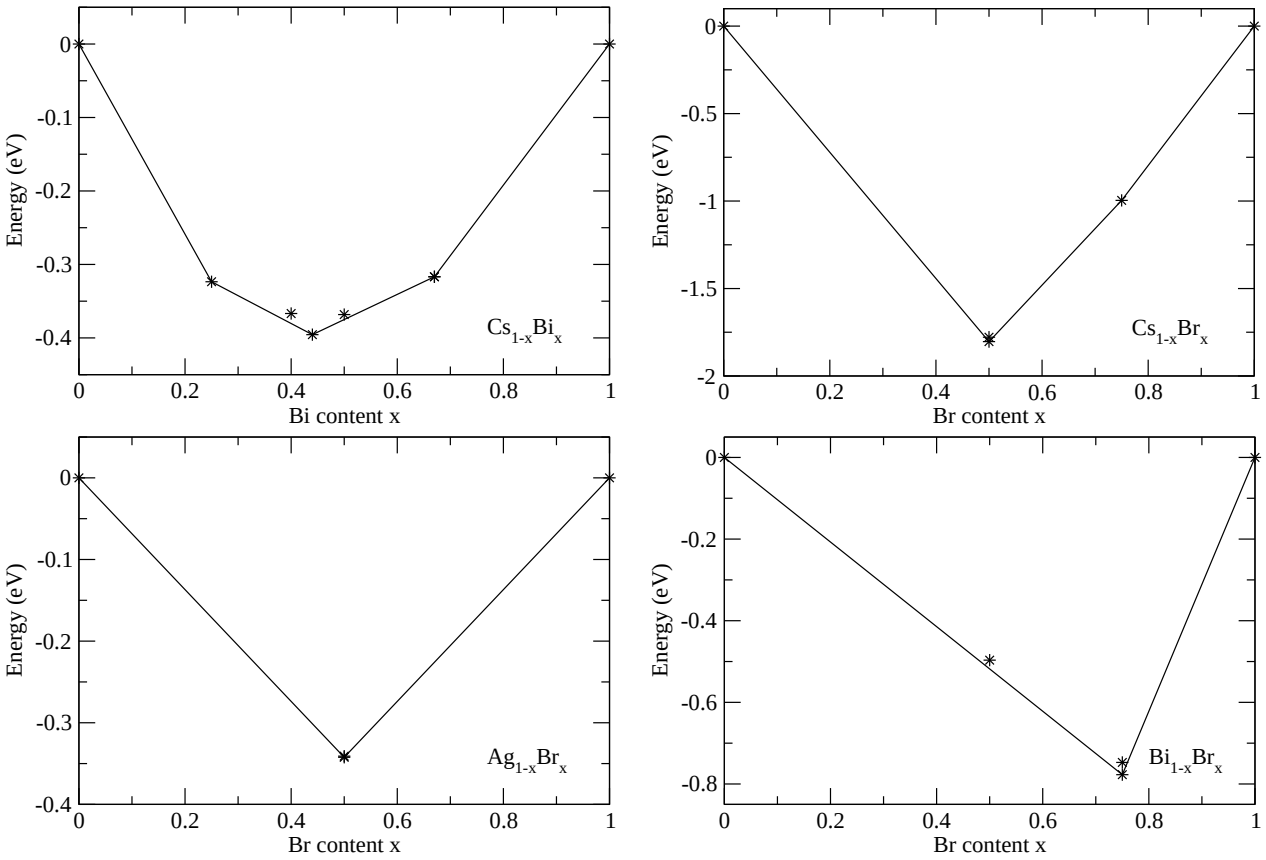

Fig. S3 Convex hull plots for the binary systems of Cs-Bi, Cs-Br, Ag-Br and Bi-Br.

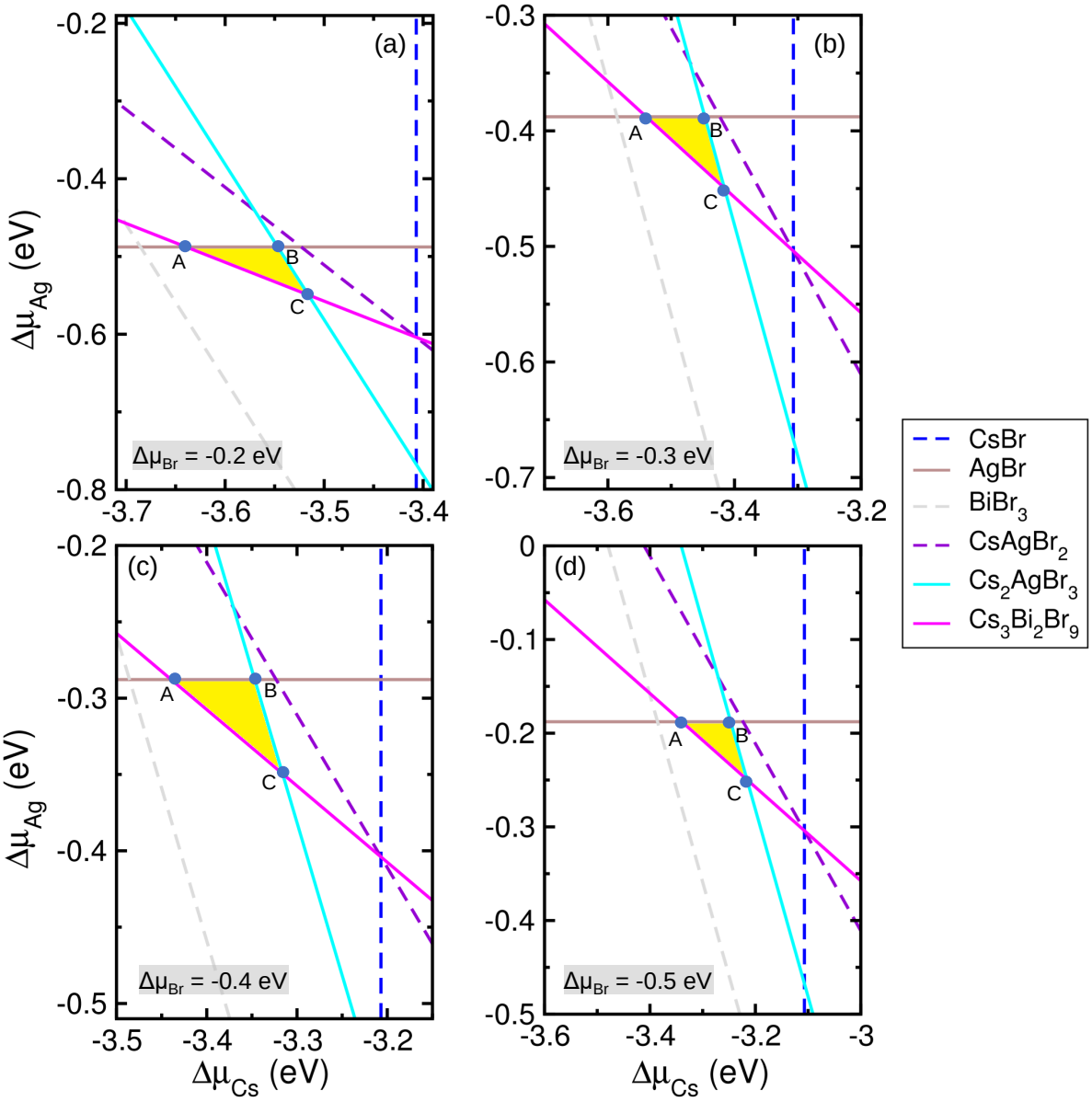

Fig. S4 Chemical potential regions of elements for stable formation of $Cs_2AgBiBr_6$ depicted by yellow-coloured triangle for (a) $\Delta\mu_{Br} = -0.2$ eV, (b) $\Delta\mu_{Br} = -0.3$ eV, (c) $\Delta\mu_{Br} = -0.4$ eV and (d) $\Delta\mu_{Br} = -0.5$ eV.

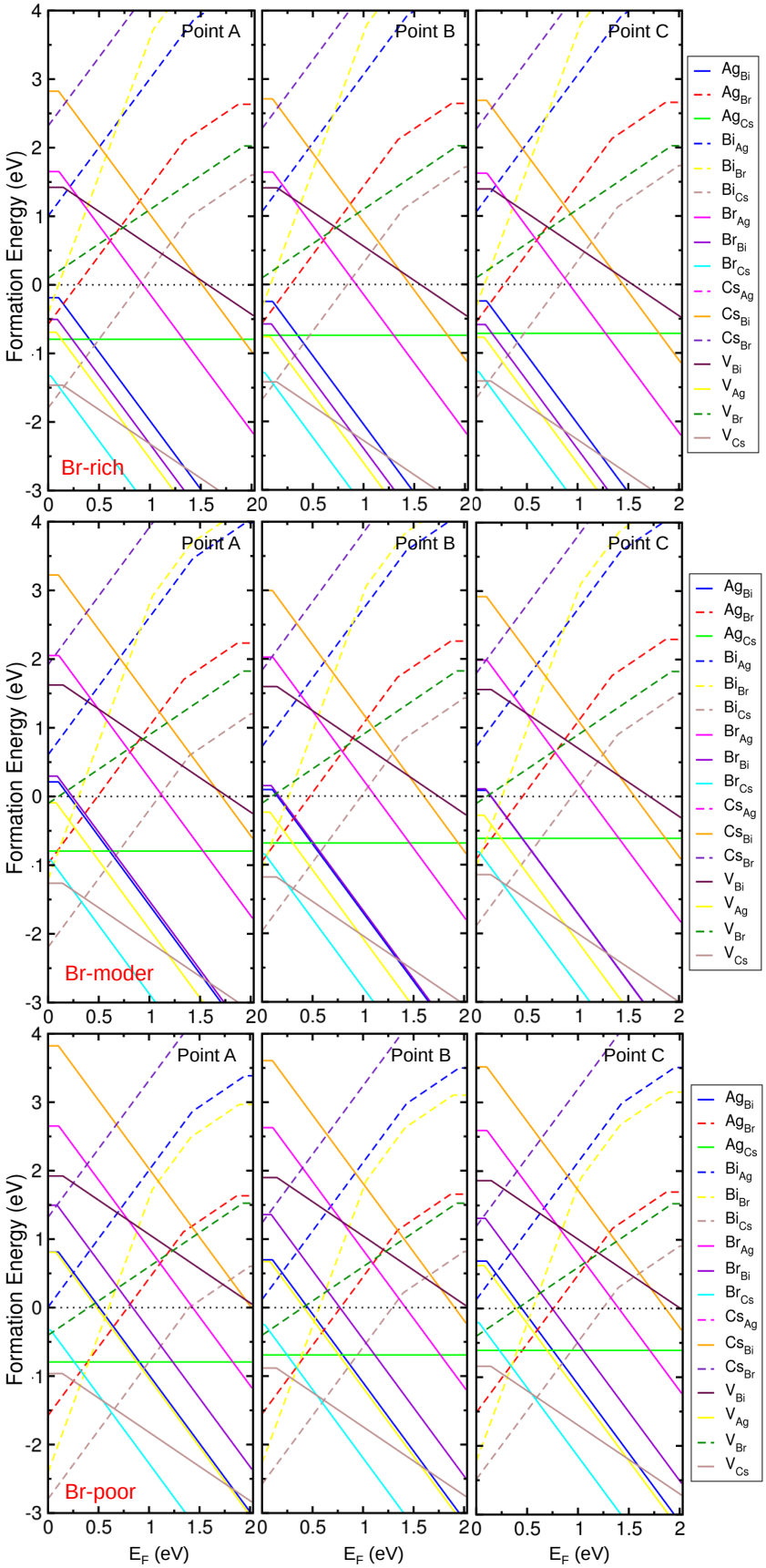

Fig. S5 Formation energies of donor-type (dashed line) and acceptor-type (solid line) defects under Br-rich (top, $\Delta\mu_{Br} = -0.1$ eV), Br-moderate (middle, $\Delta\mu_{Br} = -0.3$ eV) and Br-poor (bottom, $\Delta\mu_{Br} = -0.6$ eV) conditions. The left, centre and right panels shows the formation energies obtained at A, B and C points respectively, as indicated in Fig. S4, which correspond to Cs-poor, Cs-moderate and Cs-rich conditions. Meanwhile, the A and B points correspond to Ag-rich condition, and the C point indicates the Ag-poor condition.

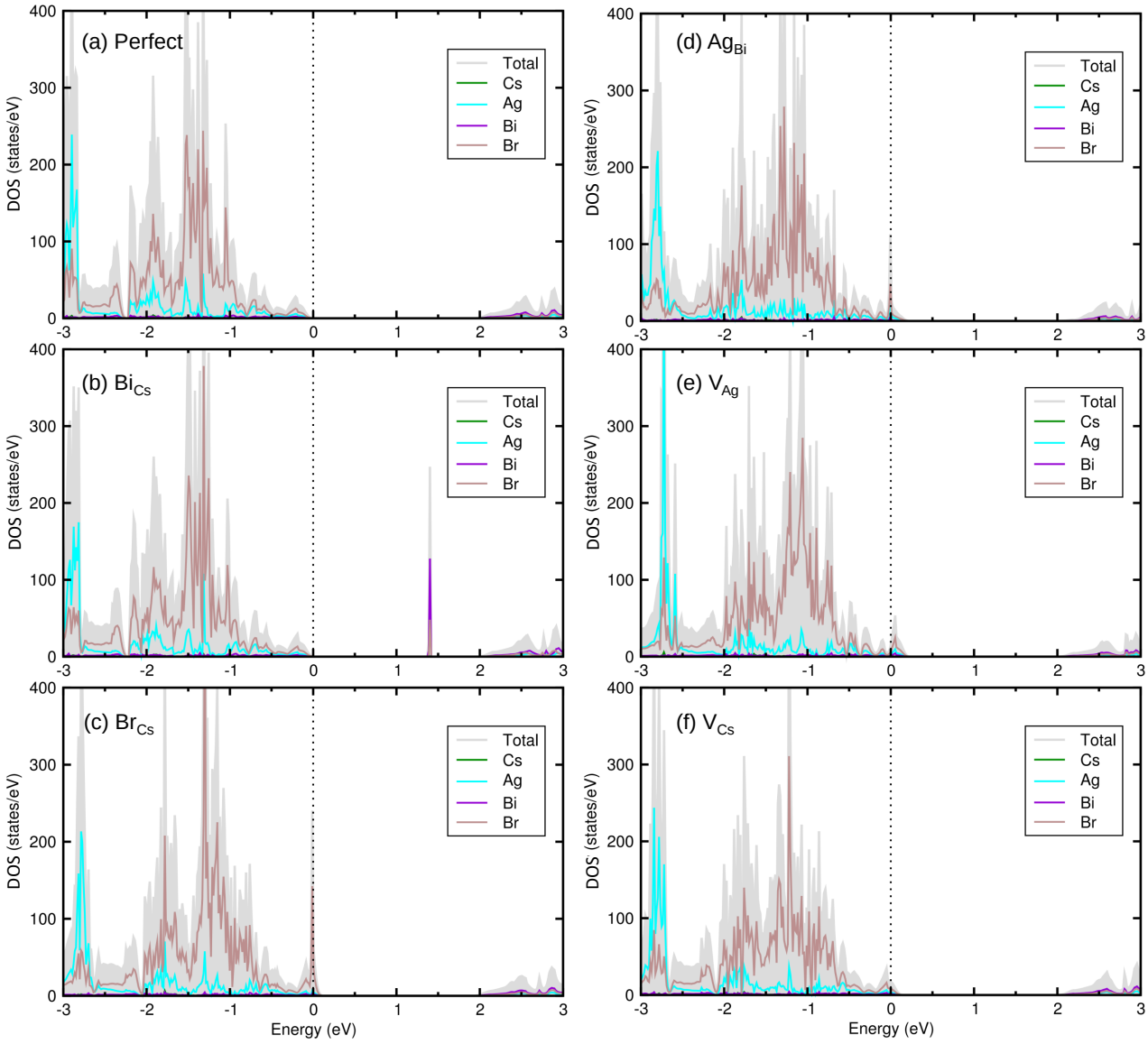

Fig. S6 Density of states (DOS) in supercells of (a) perfect system and defective systems with low formation energy defect, such as (b) Bi_{Cs}, (c) Br_{Cs}, (d) Ag_{Bi}, (e) V_{Ag} and (f) V_{Cs}. The Fermi energy is set to zero indicated by dotted vertical line. The Bi_{Cs} defective system shows the donor state at 1.4 eV, which is mainly contributed from Bi 6*p* state. Other defects, such as Br_{Cs}, Ag_{Bi}, V_{Ag} and V_{Cs}, are acceptor-type, showing the characteristic electronic states near the Fermi level (0 eV).

References

[1] P. Giannozzi, S. Baroni, N. Bonini, M. Calandra, R. Car, C. Cavazzoni, D. Ceresoli, G. L. Chiarotti, M. Cococcioni, I. Dabo, et al., QUANTUM ESPRESSO: A modular and open-source software project for quantum simulations of materials, *J. Phys.: Cond. Matter*, 2009, **21**, 395502.

[2] J. Heyd, G. E. Scuseria and M. Ernzerhof, Hybrid functionals based on a screened coulomb potential, *J. Chem. Phys.*, 2003, **118**, 8207.

[3] J. P. Perdew, K. Burke and M. Ernzerhof, Generalized gradient approximation made simple, *Phys. Rev. Lett.*, 1996, **77**, 3865.

[4] C. Freysoldt, B. Grabowski, T. Hickel, J. Neugebauer, G. Kresse, A. Janotti and C. G. Van de Walle, First-principles calculations for point defects in solids, *Rev. Mod. Phys.*, 2014, **86**, 253–305.

[5] G. Henkelman, B. P. Uberuaga, and H. Jonsson, A climbing image nudged elastic band method for finding saddle points and minimum energy paths, *J. Chem. Phys.*, 2000, **113**, 9901.

[6] G. Makov and M. C. Payne, Periodic boundary conditions in ab initio calculations, *Phys. Rev. B*, 1995, **51**, 4014.

[7] C. Freysoldt, J. Neugebauer and C. G. Van de Walle, Fully ab initio finite-size corrections for charged-defect supercell calculations, *Phys. Rev. Lett.*, 2009, **102**, 016402.

[8] K. F. Garrity, J. W. Bennet, K. M. Rabe and D. Vanderbilt, Pseudopotentials for high-throughput DFT Calculations, *Comput. Mater. Sci.*, 2014, **81**, 446–452.

[9] M. W. Chase, Jr., *NIST-JANAF Themochemical Tables*, Fourth Edition (J. Phys. Chem. Ref. Data, Monograph 9, 1998) pp. 11951.

[10] *CRC Handbook of Chemistry and Physics*, Internet Version, D. R. Lide Ed.; CRC Press: http://www.hbcpnetbase.com, Boca Raton, FL (2005).

[11] A. Jain, S. P. Ong, G. Hautier, W. Chen, W. D. Richards, S. Dacek, S. Cholia, D. Gunter, D. Skinner, G. Ceder and K. A. Persson, The Materials Project: A materials genome approach to accelerating materials innovation, *APL Mater.*, 2013, **1**, 011002.